Proceedings of IMECE2005
2005 ASME International Mechanical Engineering Congress and Exposition
November 5-11, 2005, Orlando, Florida USA

IMECE2005-80758

MODELLING CONDUCTION AND RADIATION IN REACTIVE POROUS BED OF THE GASIFIER

Sharma, Avdhesh K.
Mech. Engg. Dept., Indian Institute of Technology, Delhi, INDIA
C.R. State College of Engg., Murthal(Sonepat)-131039, INDIA
Email: avdhesh_sharma35@yahoo.co.in

Ravi, M. R.
Mech. Engg. Dept., Indian Institute of Technology.
New Delhi, INDIA

Kohli, S.
Mech. Engg. Dept., Indian Institute of Technology, Delhi
New Delhi, INDIA

ABSTRACT
This paper presents the heat transfer model for the gasifier to predict the temperature profile in the bed using the single zone sub-model. The single zone sub-model is also used to verify the correctness and to demonstrate the effect of various parameters for e.g. solid/fluid flow, temperatures of inflow/outflow control volume (CV), heat generation/absorption and with/without heat loss. The study shows that solid/fluid flow, inflow CV temperature and heat generation/absorption within the CV of interest are the strong influencing parameters, whether, the outflow CV temperature has insignificant effect on the temperature values of the CV of interest. The six similar zones correspond to preheating, drying, pyrolysis, oxidation, reduction and annular jacket zone are also coupled in order to predict the temperature profile in the gasifier bed. The simulation result shows that temperature of the down stream zones are more sensitive to heat generation in the bed as compared to upstream zone temperature, while the increase in gas flow rate resulting into the decrease in temperature profile depending upon the values of heat generation/absorption in bed is being fixed.

Key words: Modelling heat transfer, Porous bed, Producer gas, Effective thermal conductivity, Gasifier.

INTRODUCTION
Biomass gasification is a promising technology for clean and efficient utilization of biomass. So, it is important to have good understanding of the processes taking place in the gasifier and the dependence of its performance on various parameters. The temperature profile is one of the most important operating variables that determine the rates and the directions of various chemical reactions in the bed. Thus, the accuracy of prediction depends strongly on it.

The considerable work on heat transfer in packed bed has been reported in past, which can be divided into two broad categories. The first category based on the statistical analysis of the experimental data to develop the correlations for the heat transfer parameters. Thomeo and Freire[1], and Wasch and Froment[2] reported the similar work. Other category belongs to the formulation of analytical models. Some of the researchers have concentrated on conduction transport, while other concentrated on radiation transport in packed beds[4]. Kaviany[4] described the radiation transport in packed beds through four broad approaches. The first approach is based on the independent scattering, where radiative transport is assumed a point scattering phenomena and the interaction of the particle is not influenced by the presence of neighboring particles. The limitations of the theory are as $C/l>0.4$ and $C/d_p>0.4$ (i.e. bed porosity>0.73), while dependent scattering involves two different effects viz., far field interference and effect of multiple scattering in a representative elementary volume in which the scattering and absorption characteristics of the particles are affected by the proximity of other particles. Chen and Churchill[5] calculated radiant conductivity of beds of glass, aluminium oxide, steel and silicon carbide spheres, cylinders, and irregular grains using two flux radiation model. The third approach involves the Monte Carlo method to predict the radiative heat transfer in packed beds using ray tracing approach. Singh and Kaviany[6] extended the Monte Carlo technique to accommodate emitting particles as well as semi-transparent particles. The fourth category is based on radiative exchange factor approach. The most important and crucial part of this approach is to calculate the exchange factor (Vortmeyer[7]). Wakao and Kato[8] derived the expressions for radiative shape factor, they obtained effective thermal conductivity using relaxation method and found in good agreement with experimental data.

Slavin et. al.,[9] modelled the combined effect of conduction and radiation in packed beds of alumina spheroids (filled with ideal gas) in terms of effective thermal conductivity.

In present work, the modelling of complex phenomenon of heat transfer in the granular bed of gasifier using effective thermal conductivity approach is presented in order to predict the accurate temperature profile in the gasifier bed.

NOMENCLATURE

A	Cross-sectional area of tube
C	Average interparticle spacing
D_T	Bed diameter
D_{mn}	Imaginary diameter in bed (D_{mn}=5 mm)
Ds	Outer diameter of wall
dL_I	Length (thickness) of CV_I
h	Heat transfer coefficient
k	Thermal conductivity
l_{cl}	Length of representative unit cell
m	Mass flow rate
Rs_I	Axial thermal resistance of CV_I
Rse_I	Equivalent resistance in radial direction of CV_I
S	Specific gravity
so	Outer surface of reactor
T	Temperature
Y	Mass fraction in dry biomass

Greek letters

ρ	Density
σ	Stefan-Boltzmann constant
ϵ_r/ϵ_b	emissivity/ bed porosity
l	Wavelength dependent

Subscripts

ao/ai	denote the annulus wall (outer /inner)
A	Atmospheric condition
Ash	Ash
b/bd	Bed or biomass/dry biomass
Char	Char
ct	Contact of two particles
c/r	Conduction/radiation transport
mx	Maximum limit
P/p	Producer gas /particle
Vol/w	Volatile/ water vapour
sg/ss	Solid-fluid-solid contact/solid-solid contact
Ins	Thermal insulation

Superscripts

pyr	Pyrolysis zone
oxd	Oxidation zone
red	Reduction zone

MATHEMATICAL MODELLING

The open top downdraft biomass gasifier of capacity 20kWe developed by Sharan et. al [10] at Indian Institute of Sciences, Bangalore is selected for our study. Here the air enters from top as well as from radial tuyers and the producer gas exits from the bottom of the reactor. The gas is then made to pass through an annulus around preheating zone so as to utilize a part of its heat for preheating of biomass. The outer wall of the gasifier is insulated to improve the thermal efficiency of reactor. The packed bed in a biomass gasifier is modelled as a porous medium in which fluid flow increases in the direction of flow due to gasification of the particles constituting the bed. The flow of air and biomass consumption in a biomass gasifier is closely coupled with fluid flow and thermo-chemical processes, viz., preheating, drying, pyrolysis, combustion and reduction process. Thus for simplicity, the gasifier is divided into six successive zones (I=1..6), each one corresponding to a dominant phenomenon as: preheating, drying, pyrolysis, oxidation, reduction and heat recovery as shown in figure 1. The preheating, drying and annular jacket zones are further divided into 3 control volumes each; and the pyrolysis zone is divided into 2 control volumes. The bed is assumed to be isotropic, solid and gas are considered to be in thermal equilibrium. Within the control volumes, the particle size, bed porosity and temperature are assumed to be uniform. For model formulations following assumptions have been made:

Drying/Preheating zone

1. The particles are spherical with equal diameters.
2. No shrinkage in particle due to moisture evaporation.
3. Moisture is completely removed from solid to gas phase.

Pyrolysis zone

4. Particle size shrinks in order to reduce to char and ash.
5. All volatiles leave solid and go to gaseous phase.
6. Neglect heat of pyrolysis.

Oxidation zone

7. Fraction of char consumed in oxidation zone is a parameter determining the particle diameter.
8. Oxygen is completely consumed in oxidation zone.

Reduction zone

9. All char is consumed in reduction zone

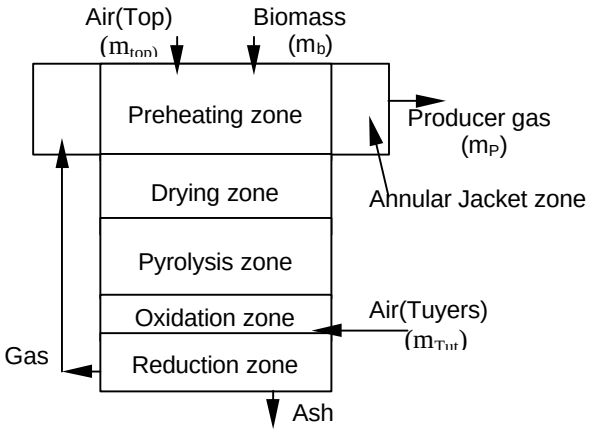

Figure 1. Zonal description of the gasifier

Particle Size Variation

For modelling, each zone can be characterized by its bulk temperature, flow rate, diameter of the reactor and size of particles in each zone. In the drying and preheating zones, there is no change in the diameter. However in pyrolysis, oxidation and reduction zones, feedstock undergoes chemical reactions leading to change in the particle size. Thus, in wet biomass, the fraction of dry biomass and moisture can be presented as

$$Y_{db} + Y_{w} = 1 \quad \textbf{(1)}$$

Biomass pyrolysis is modelled by taking into account the release of volatile, char and ash as

$$Y_{Vol} + Y_{Char} + Y_{Ash} = 1 \quad \textbf{(2)}$$

As wood converts into char due to pyrolysis, its size reduces and its diameter at exit of pyrolysis zone can be given by

$$d^{pyr}_{Char} = d_b \, (Y_{Char} \, \rho_b / \rho_{Char})^{1/3} \quad \textbf{(3)}$$

In oxidation zone, char is consumed to form gases. Particle size of char at the exit of this zone is given by

$$d^{oxd}_{Char} = d_b \, [Y_{Char} \, (1-\lambda^{oxd}_{Char}) \, (\rho_b/\rho_{Char})]^{1/3} \quad \textbf{(4)}$$

$$\lambda^{oxd}_{Char} + \lambda^{red}_{Char} = 1 \quad \textbf{(5)}$$

Here, λ^{oxd}_{Char} denotes that fraction of the total char that gets consumed in the oxidation zone, while λ^{red}_{Char} is the fraction consumed in the reduction zone. It is assumed that the entire

char gets consumed during the reduction process and hence only ash particles leave the reduction zone.

Porosity variation

Chen et al.[11] reported the correlation for bed porosity ϵ_b by accounting for effect of deposition of ash particles in void space, as solid particles are consumed progressively.

$$\epsilon_b = 0.5 - 0.2\,(1 - d_p/d_b) \quad \textbf{(6)}$$

Here, d_b is the initial particle diameter, while d_p is the particle diameter at any stage of charring or gasification in the bed.

Modelling Effective thermal conductivity

The modelling of effective thermal conductivity, $k_{eff,}$ is based on the work reported by Cheng et al[3], Slavin et al[9] and Kaviny[4]. The sub-model is used to predict the k_{eff} as a function of bed temperature, particle size, particle emissivity and thermal conductivity of working substance. For the model formulation it is assumed that the particles in gasifier bed are spherical with equal diameter. The description of two contacting particles model is given in figure 2.

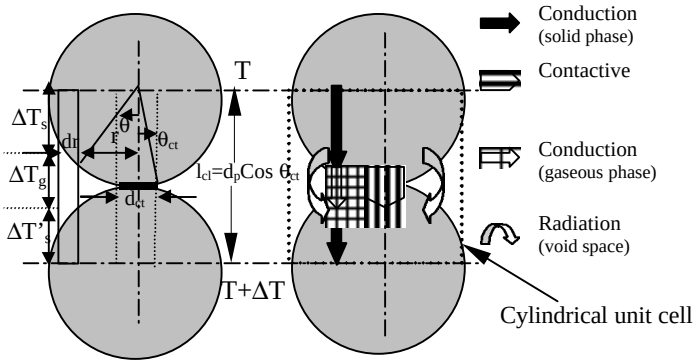

Figure 2. Model of two contacting particles in the unit cell.

(a) Conduction

For conduction modelling, heat flows in straight and parallel lines through different pathways (since the conductivity of gas and solid are comparable in present case). Thus, the heat flow through solid-gas-solid contact in the unit cell is written as

$$k_s\,\Delta T_s \int 2\pi r\,dr/((d_p/2)\cos\theta) = k_{eff,\,sg}\,A_{cl}\,\Delta T / l_{cl} = k_g\,\Delta T_g \int 2\pi r\,dr/(d_p(1-\cos\theta)) \quad \textbf{(7)}$$

Here, $k_{eff,\,sg}$ represents the contribution of conduction at solid-fluid-solid interface in k_{eff}. $r = (d_p/2)\sin\theta$, here θ is polar angle. The temperature drop in solid-gas-solid interface in unit cell can be written as

$$\Delta T = \Delta T_s + \Delta T_g + \Delta T'_s \quad \textbf{(8)}$$

Integrating equation (7) for integration limit, $\theta = \theta_{ct}$ to θ_{mx} and solving with equation (8) for $k_{eff,\,sg}$, thus, we get

$$k_{eff,\,sg} = \frac{2\{k_s k_g[l_{cl}\ln(A/B) - d_p(A-B)]\}}{\{k_g[l_{cl}\ln(A/B) - d_p(A-B)] + k_s l_{cl}\}} \quad \textbf{(7a)}$$

Here, $d_{ct}=d_p\sin\theta_{ct}$; $l_{cl}=d_p\cos\theta_{ct}$; $A=1-\cos\theta_{mx}$ and $B=1-\cos\theta_{ct}$. θ_{mx} is taken as 98°, while the value of θ_{ct} is based on particle contact.

Enoeda considered the contact radii of typically 0.7% of particle diameter[9], which is small as compared to particle diameter and the distribution of temperature inside the two particles is approximately same as that of velocity potential in irrotatinal flow of incompressible fluid through a circular hole in a plane wall. Based on this argument Batchelor and O'Brien [12] obtained a relation to calculate the heat transfer at the point of contact of two particles

$$k_{eff,\,ss}\,A_{cl}\,\Delta T / l_{cl} = k_s\,d_{ct}\,\Delta T \quad \textbf{(9)}$$

Thus,

$$k_{eff,\,ss} = d_{ct}\,l_{cl}\,k_s/A_{cl} \quad \textbf{(9a)}$$

(b) Radiation modelling

As the condition of independent scattering is not fulfilled, the radiative exchange factor approach followed by scaled properties is employed. Vortmeyer[7] defines the radiative heat transfer (Q_r) in packed bed, assuming a one-dimensional, plane geometry with emitting particles under the steady state condition as

$$Q_r = [F\,\sigma/\{(1+\rho_w)/(1-\rho_w) + L_b/d_p\}]\,(T^4 - (T+\Delta T)^4) \quad \textbf{(10a)}$$

Where F is called shape factor or radiative exchange factor and the properties are assumed to be wavelength-independent. If reflectivity at wall, ρ_w, is zero, the bed is several deep, then first term of the denominator can be neglected. Then, for $\Delta T<200$ K, Tein and Drolen [13] defined the radiant conductivity as

$$k_{eff,\,r} = 16\,\sigma\,T^3/(3\,\langle\sigma_{ex}\rangle) = 4\,F\,d_p\,\sigma\,T^3 \quad \textbf{(10b)}$$

Thus, $F=4/(3<\sigma_{ex}>d_b)$, and $<\sigma_{ex}>$ is the extinction coefficient. Chen and Churchill[5] reported shape factor as $2/(a+2s)d_p$, where, a and b are absorption and scattering coefficients. Kamiuto and Yee[14] proposed the scaled extinction coefficient ($<\underline{\sigma}_{ex}>$) for large opaque particles in bed as

$$<\underline{\sigma}_{ex}> = (1-1/2\gamma)<\sigma_{ex}> = 1.5\,(2\gamma-1)(1-\epsilon_b)/d_p \quad \textbf{(11)}$$

Where, $\gamma = 1+1.5(1-\epsilon_b)-0.75(1-\epsilon_b)^2$ for $\epsilon_b<0.921$. In our case, however, σ_{ex} varies from 61-93 (m^{-1}), while $\underline{\sigma}_{ex}$ varies 42-65(m^{-1}) for the corresponding variation in bed porosity from0.5 to 0.3. For the case of intermediate conductivity materials, the radiant conductivity shows a strong dependence on the solid conductivity. For opaque spherical particles having diffusive surface and assuming radiant conductivity is insensitive to bed porosity, F is given in terms of dimensionless solid conductivity, $k_s^*(=k_s/(4\,d_p\,\sigma\,T^3)$ as[4]

$$F = 0.5756\,\epsilon_r \tan^{-1}\{(1.5353(k_s^*)^{10.8011}/\epsilon_r\} + 0.1843 \quad \textbf{(12)}$$

Many models are available to predict F and are compared in figure 3. In this work, the expression of Tein and Drolen [13] for radiative exchange factor is employed using the scaled extinction coefficient as proposed by Kamiuto and Yee[14].

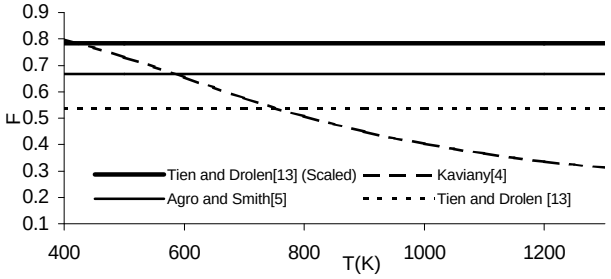

Figure 3. Radiative exchange factors versus temperature

For optically thick packed beds the internal radiant conductivity can be treated as a conductive process [5]. Thus

$$k_{eff} = k_{eff,\,c} + k_{eff,\,r} = (k_{eff,\,sf} + k_{eff,\,ss})_c + k_{eff,\,r} \quad \textbf{(13)}$$

Thermal Resistance Network

Each control volume (CV) in the gasifier bed is accounted for radial and axial heat blast as shown in figure 4. The thermal resistance to radial heat blast (heat loss through the reactor wall), Rse, can be generalized for each CV of the each zone as

$$Rse_I = \ln(D_T/D_{mn})/(2\,\pi\,k_{eff}(T_I)\,dL_I) + \ln(D_T/Ds)/(2\,\pi\,k_{Ins}\,dL_I) + 1/(\pi\,Ds\,dL_I\,hso) \quad \textbf{(14)}$$

In the above equation (14), first, second and third term denote the thermal resistance offered by granular bed, thermal insulation at wall, convective resistance at outer wall.

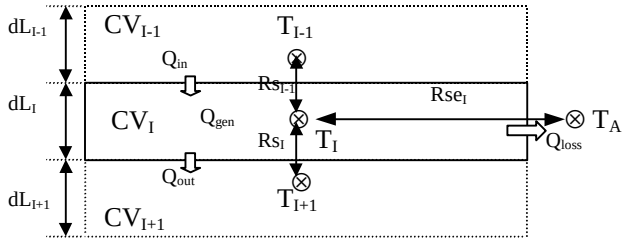

Figure 4. Thermal resistance network for the control volume

Thermal resistance for preheating and annular jacket zone is modelled separately. Since, the major fraction of heat is recovered in preheating the biomass, while the few part of heat is lost to the surroundings through wall. Thus, the resistance for preheating the feedstock for each CV can be written as

$$Rse_1 = \ln(D_T/D_{mn})/(2\pi\,k_{eff}(T_1)\,dL_1) + 1/(\pi\,D_T\,dL_1\,h_{ai}) \quad \textbf{(15a)}$$

Thermal resistance to heat loss from the annular jacket zone to surrounding is modelled for each CV as

$$Rse_6 = 1/(\pi\,D_{ao}\,dL_6\,h_{ao}) + \ln(D_{ao}/Ds)/(2\,\pi\,k_{Ins}\,dL_6) + 1/(\pi\,Ds\,dL_6\,hso) \quad \textbf{(15b)}$$

Heat blast in the bed has been modelled using the thermal resistance in axial direction at the inlet and outlet boundaries of the each CV. Thus

$$Rs_{I-1} = 1/2\,[dL_{I-1}/k_{eff}(T_{I-1}) + dL_I/k_{eff}(T_I)]/A_{I-1} \quad \textbf{(16)}$$

SINGLE ZONE HEAT TRANSFER SUB-MODEL

Single zone sub-model is accounted for all heat transfer mechanisms in gasifier bed for e.g. axial heat blast and radial heat loss using variable thermal resistance in the bed. The mass and energy equation for each CV is modelled in algebraic form as shown in figure 5.

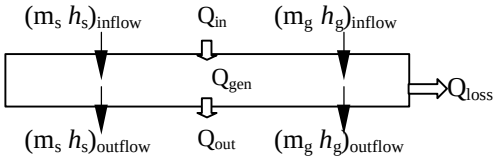

Figure 5. Mass and Heat interactions for the control volume

Thus the mass balance is written as

$$[m_s+m_g]_{inflow} = [m_s+m_g]_{outflow} \quad \textbf{(17)}$$

Here some mass from the solid is converted to gaseous phase either by evaporation, pyrolysis, oxidation or reduction process.

The model is accounted for advective, conductive and radiative heat fluxes at boundaries of the porous bed in each CV. The axial fluxes are accounted for the heat transfer between various CVs while the radial fluxes are accounted for the heat loss to the surroundings. The advective heat transfer is considered due to flow of gas (m_g) and solid (m_s) across the boundaries of the CVs as shown in figure 5. Thus, for each CV of each zone, the energy equation is written as

$$[m_s\,h_s + m_g\,h_g]_{inflow} + Q_{in} - Q_{out} - Q_{loss} + Q_{gen} = [m_s\,h_s + m_g\,h_g]_{outflow} \quad \textbf{(18)}$$

Here $h = \int Cp\,dT$, is the sensible enthalpy change with respect to surroundings, it comprises of solid phase (biomass, char and ash) and gaseous phase (water vapour, volatiles, air and combustion products). Heat loss to the surroundings, Q_{loss}, is modelled in terms of equivalent thermal resistance, Rse, which is obtained from resistance network (figure 4).

$$Q_{loss} = (T_I - T_A)/Rse \quad \textbf{(18a)}$$

Within each CV, Q_{in} and Q_{out} are the energy in and out flowing by conduction and radiation, and are modelled as

$$Q_{in} = (Q_c + Q_r)_{in} = (-k_{eff}\,A\,\nabla T)_{in} = (T_{I-1} - T_I)/Rs_{I-1} \quad \textbf{(18b)}$$

Q_{gen} denotes the heat generation/absorption and depends on the process in a control volume: drying results in absorption of latent heat of vaporization, pyrolysis results in release/absorption of heat of pyrolysis, oxidation or reduction processes results the heat generation or absorption due to thermochemical conversion. In this work the information Q_{gen} is supplied externally and specific heat (Cp) of air is used for gaseous phase. However, in detailed gasifier model Q_{gen} is obtained from the energetics model and Cp of volatile, gas products are obtained from the gas composition.

For preheating zone, energy balance is similarly written. Heat recovery form the annular jacket zone (in place of heat loss) is considered taking into account for the temperature T_6, in place of $T_{A,}$ in energy equation and the heat transfer coefficients on the corresponding wall of annulus is employed from the literature[15]. For annular jacket zone, the mass of gas inflow and outflow the CVs is same, heat loss to preheat zone and to atmosphere are considered.

The resulting set of mass balance equation (17), energy equation (18) coupled with various thermal resistance equations (14)-(16) is solved to obtain the temperature in the control volume. Moreover, the coupling of these six zones, involves the solution of 13 more control volumes. For this, mass balance is obtained from the solid conversion for each CV, which is obtained from table 1 using equation (1) (2) and (5), for $\lambda^{oxd}_{Char} << \lambda^{red}_{Char}$. Thus, the system of equations for 13 CVs is solved simultaneously using Gauss-Siedel iteration of convergence to predict temperature profile in the bed.

PROPERTY DATA

Thermal conductivity (W/mK) of char and biomass are given as [16]

$$k_{Char} = 0.67\,S_{char} - 0.071 \quad \textbf{(19a)}$$

$$k_b=S_b(0.1941+0.4064Y_w)+0.1864+0.002(T-T_A) \quad \textbf{(19b)}$$

Specific heats (kJ/kg-K) for biomass and char are obtained from literature[16], while specific heat for working fluid (air) is obtained by curve fit to data of Keenan[15]

$$Cp_{bd}=0.1031+0.003867\ T \quad \textbf{(20a)}$$

$$Cp_b=[Cp_{bd}+4.19Y_w]/(1+Y_w)+.02355T-1.32Y_w-6.2)Y_w \quad \textbf{(20b)}$$

$$Cp_{Char}=1.39+0.00036\ T \quad \textbf{(20c)}$$

$$Cp_{Air} \cong Cp_g=0.931+0.0002\ T-1.01\times10^{-8}\ T^2 \quad \textbf{(20d)}$$

The relation of Cp_{Air} is valid for 300 K<T<1500 K with R^2 =0.99. The proximate analysis of biomass is given in table 1.

Table 1: Proximate analysis of biomass

Y_{Char}	Y_{Vol}	Y_{Ash}	Reference
0.20	0.79	0.01	[16]

RESULTS AND DISCUSSION

The above model predicts the temperature profile in the bed of a downdraft (biomass) gasifier for the desired mass flow rate of gas at the exit, equivalence ratio and heat generation/absorption in oxidation/ reduction zones. This model is also used to predict temperature of CV of interest (T_I) surrounded by two neighboring CVs in the porous bed of char particles filled with air. These neighboring CVs thermally interacts with CV_I. The results of the model are used to verify the correctness of the model and to demonstrate the effect of various interactions for uniform distribution of char particle size of 38 mm.

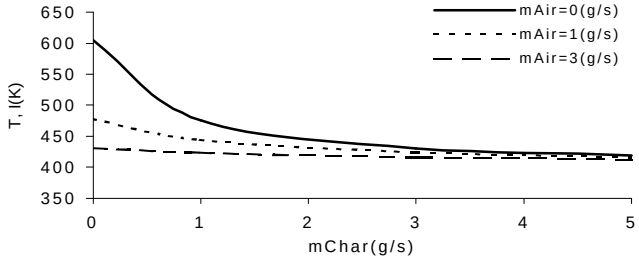

Figure 6. Effect of m_{Char} and m_{Air} on T_I, T_{I-1}=400K, T_{I+1}=700K, $dL_{I-1}=dL_I=dL_{I+1}$=0.1m, without heat loss.

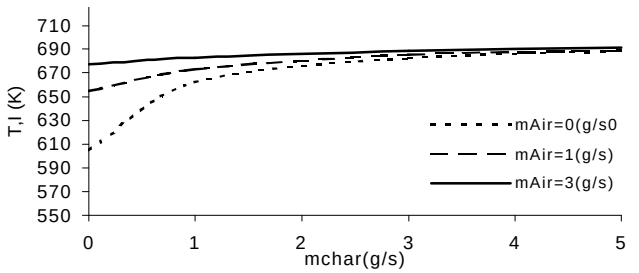

Figure 7. Effect of m_{Char} and m_{Air} on T_I, T_{I-1}=700K, T_{I+1}=400K, $dL_{I-1}=dL_I=dL_{I+1}$=0.1m, without heat loss.

Figure 6 and 7 depicts the effect of heat blast in the bed, solid and fluid flow rate on T_I. The effect of heat blast on T_I is also demonstrated for zero solid and air flow rates. The graphs show the T_I attains the value of 602 K in both above cases, which is slightly higher than the mean of the temperatures of the neighboring CVs (530K). It is because of the domination of heat blast from higher temperature CV. The CV having higher temperature allows more heat transfer in radiation mode and thus increases the T_I slightly higher value from the mean of the T_{I-1} and T_{I+1}. The effect of heat flow due to advection on the T_I is also demonstrated in figure 6, 7. For both cases, the T_I is found stronger function of the inflow CV temperature (T_{I-1}) as compared to the outflow CV temperature (T_{I+1}) specially at higher flow rates. As m_{Air} or m_{Char} increases, the heat transport due to advection increases and thus the T_I approaches towards inflow temperature T_{I-1} at high flows.

Figure 8 depicts the effect of heat generation Q_{gen} on T_I. The graph shows almost linear relationship between the heat generation/absorption and temperature T_I. The typical increase of 1 kW in heat generation results in the increase of the temperature of intermediate zone by 130K. No any significant variation is observed for both heat loss or without heat loss conditions. It is due to the fact that effect of heat loss is very small as compared to heat generation inside the control volume. The effect of variation in T_{I-1}, on T_I is also shown in figure 9. A linear relationship between the two is predicted from the model.

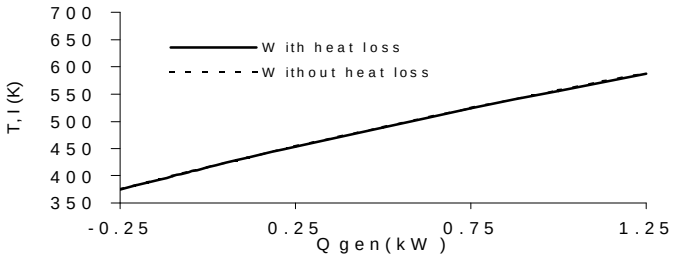

Figure 8 Effect of Q_{gen} on T_I, m_{Air}= m_{Char}=3g/s, T_{I+1}=700K,$dL_{I-1}=dL_I=dL_{I+!}$=0.1m, with/without heat loss

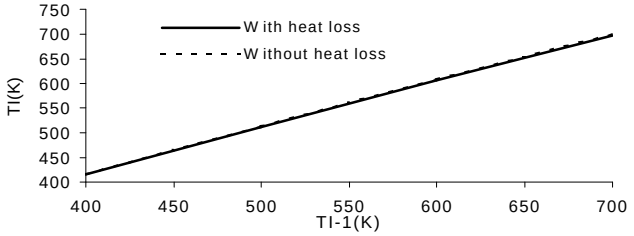

Figure 9 Effect of T_{I-1} on T_I, m_{Air} = m_{Char}=3g/s, T_{I+1}=700K, with /with out heat loss

In order to synthesize a realistic gasifier model, the complete kinetics and energetics of the pyrolysis, oxidation and reduction is required, which is beyound the scope of this paper, since only the energy equations are solved and mass balance are obtained from the parameters. Therefore, in the present work, heat generation/absorption in pyrolysis zone is neglected and heat generation in oxidation zone, $Q_{gen,4}$, heat absorption in reduction zone, $Q_{gen,5}$, gas flow at exit, m_P, equivalence ratio, ϕ, are fixed at their base values of 7.5kW, -2.5kW, 5g/s, and 0.37 respectively.

With these base values and for spatially varying particle size distribution for d_b value of 38 mm (equation(3)-(5)), the simulations are performed to predict the effect of $Q_{gen,4}$ and $Q_{gen,5}$ on temperature profile as shown in figure 10 and 11. It is demonstrated that the $Q_{gen,4}$ is not only dominates the temperature of oxidation zone but also the temperature of reduction zone. The overall temperature profile improves

sharply with increase in $Q_{gen,4}$, a typical increase of 1kW in $Q_{gen,4}$ increases in temperature of 75K in the oxidation zone. However, the effect of heat absorption in the reduction zone as depicted in figure 11, does not observe any significant effect on the temperature in oxidation, pyrolysis and drying zone.

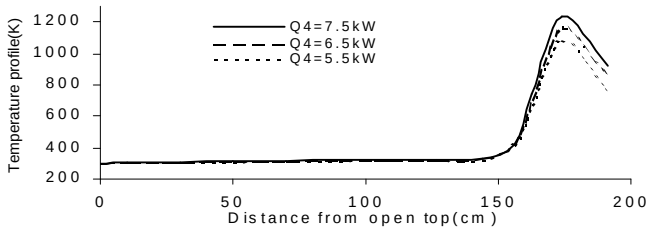

Figure 10 Effect of $Q_{gen,4}$ on the Temperature profile, m_P =5 g/s, ϕ=0.37, m_{Top} = 0.6 m_{Air}, $Q_{gen,5}$ = -2.5kW, Heat Loss.

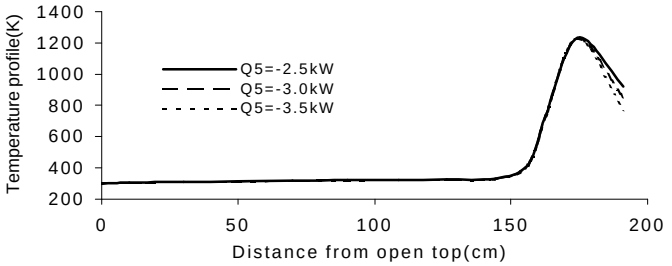

Figure 11 Effect of Q_5 on temperature profile, m_P =5 g/s, ϕ=0.37, m_{Top}=0.6m_{Air}, $Q_{gen,4}$ =7.5kW, Heat Loss.

Figure 10 and 11 depicts the effect of Q_{gen} on the temperature profile in down stream (viz., oxidation, reduction and annular zones) increases considerably as compared to the upstream (viz., pyrolysis, drying and preheating zones) with this increase in heat generation/absorption. It is because the major apportionment of the heat generation in a zone transported downward due to advection, thus dominates the temperature in down stream in gasifier bed.

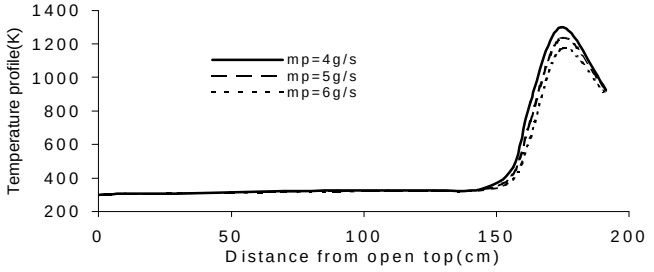

Figure 12. Effect of m_P on temperature profile, ϕ=0.37, m_{Top} = 0.6m_{Air}, $Q_{gen,4}$ =7.5kW, $Q_{gen,5}$=-2.5kW, Heat Loss.

Figure 12 depicts the effect of gas flow rate at the gasifier exit (m_P) on the temperature profile. It is seen that for any increase in m_P, the considerable decrease in the temperatures of pyrolysis, oxidation and reduction zone of the gasifier.

In above calculations, thickness of insulation at wall, diameter and length of reactor is taken as 27cm, 25cm and 2m respectively and the fraction of air coming from open top is fixed at 60% of the total air required for gasification[17].

CONCLUSIONS

The temperature profile in the gasifier bed is presented using single zone sub-model. The results shows that heat generation, flow rates, and temperature of inflow zone are the sensitive parameters that dominate the temperature of the intermediate control volume (T_I). The T_I shows a linear relationship with the case of varying temperature of the inflow CV, (T_{I-1}). However, the effect of temperature of outflow CV, (T_{I+1}) on the T_I is found insignificant.

The simulation results of heat transfer model for gasifier bed by combining the six zones (thirteen control volumes); preheating, drying, pyrolysis, combustion, reduction and heat recovery processes revealed that downstream zones are very sensitive to any change in heat generation or absorption as compared to upstream zones. However, the increase in gas flow rate shows the corresponding decrease in the temperature profile in the bed, if the heat generation/absorption in each zones is fixed. However, in actual operating condition, heat generation/absorption in gasifier is a strong function of gas flow rate itself.

REFERENCES

1. Thomeo, J.C., and Freire, J.T., 2000, 'Heat transfer in fixed bed: a model non-linearity approach', *Chem. Engg Sc*, Vol. 55, p. 2329.
2. Wasch P.D., and Froment, G.F., 1972, 'Heat Transfer in Packed Beds', *Chem. Engg Sc.*, p 567.
3. Cheng, G.J., Yu, A.B., and Zulli, P., 1999, "Evaluation of Effective thermal conductivity from the structure of a Packed bed", *Chemical Engg. Sc.*,54, pp. 4199-4209.
4. Kaviany, M., 1995, "Principles of Heat Transfer in porous media", Springer, Berlin.
5. Chen, J.C., and Churchill, S. W., 1963 'Radiant Heat Transfer in Packed Beds', *AIChEJ*, Vol 9, p79-81.
6. Singh, B.P., and Kaviany, M., 1991, "Independent theory Versus direct simulation of radiation heat transfer in packed beds", *Int. Journal of Heat and Mass Transfer*, Vol. 34, No. 11, pp. 2869-2882.
7. Vortmayer, D., 1978, "Radiation in packed solids", *Proceedings of 6th Int. Heat Transfer conference*, Toronto, Canada, 6, p. 525-539.
8. Wakao N., and Kato, K., 1969, "effective Thermal Conductivity in packed beds", *Journal of Chemical Engg. of Japan*, pp. 24-33.
9. Slavin, A.J., Arcas, V., Greenhalgh, C.A., and Irvine, E.R., and Marshell, D.B., 2002, *Int. J of Heat & Mass Transfer*, 45, p. 4151.
10. Sharan, H.N., Mukenda, H.S., Shrinivasa, U., and Dasappa, S., 1997, 'IISc-DASANG biomass gasifiers: Development, Technology, Experience & economics', *Dev. in Thermochemical Biomass conversion*, IEA Bioenergy, Vol 2, p. 1058-73.
11. Chen, J., and Gunkel, W.W., 1987, "Modelling & Simulation of cocurrent Moving Bed Gasification Reactors-Part II. A Detailed Gasifier Model', *Biomass* Vol. 14, p. 75-98.
12. Batchelor, G.B. and O'Brien R.W., 1977, "Thermal or electrical conduction through a grannular material", *Proceedings of Royal Society of London*, A355, 313-333.
13. Tein C.L., and Drolen, B.L., 1978, "Thermal Radiation in particulate media with dependent and independent scattering", *A Rev. Numer. Fluid Mech. Heat Transfer*, 1, 1-32.
14. Kamiuto, K., and Yee, S.S., 2005, "Correlated radiative transfer through a packed bed of opaque spheres", Int. Comm. in heat transfer, 32, pp. 133-139.
15. Kakac, S., Shah, R.K., and Aung, W., 1987, *Handbook of Single-Phase Convective Heat transfer*, John Wiley & Sons, N. Y.
16. Ragland, K. W., Aerts, D. J., 1991, 'Properties of Wood for Combustion Analysis', Bioresource Tech., Vol. 37,p161-68.
17. Sharma, A.K, Kohli, S., and Ravi, M.R., 2004, 'Modelling of Fluid Flow in a Downdraft Biomass Gasifier', *Proceeds of 2nd BSME-ASME Int. Conf. on Thermal Engg*, Vol-2, p. 861-66, BUET, Dhaka.